Polymer Chemistry

PAPER

View Article Online
View Journal | View Issue

Cite this: *Polym. Chem.*, 2018, **9**, 517

Poly(*N*-acryloylglycinamide) microgels as nanocatalyst platform†

Dong Yang, Milla Viitasuo, Fabian Pooch, Heikki Tenhu and Sami Hietala *

Received 21st November 2017,
Accepted 2nd January 2018

DOI: 10.1039/c7py01950e

rsc.li/polymers

We report the synthesis of thermophilic poly(*N*-acryloylglycinamide) (PNAGA) microgels that swell in water upon heating and their use as nanocatalyst hosts. The microgels are prepared by aqueous precipitation polymerization below the UCST phase transition temperature of PNAGA. The diameters of the PNAGA microgels are around 60 nm in cold water and they show reversible swelling and shrinking upon change of temperature. Silver nanoparticle (AgNP) loaded microgels were prepared by reduction of $AgNO_3$ and their catalytic activity in 4-nitrophenol reduction was tested under different conditions. The thermophilic behaviour of the PNAGA microgels was retained after nanocatalyst synthesis and the catalytic activity in 4-nitrophenol reduction by AgNPs increased especially at temperatures above 30 °C. Furthermore, it was shown that the catalytic activity of the thermosensitive AgNP–PNAGA microgels could be switched on and off by changing the temperature.

Introduction

Aqueous stimuli-responsive microgels exhibiting volume phase transition temperature (VPTT) are actively studied for various applications including controlled drug release, sensors, separations and catalysis.[1–6] For catalysis applications the polymeric microgels have been used as carriers for mostly silver[4,7–12] and gold[13–15] nanoparticles (AgNPs and AuNPs, respectively). By far the most studied stimuli-responsive polymer employed as a carrier has been poly(*N*-isopropyl acrylamide) (PNIPAM). PNIPAM exhibits lower critical solution temperature (LCST)-type behaviour, which in the case of microgels leads to shrinkage of the particles upon heating, often called volume phase transition temperature (VPTT). The colloidal nature of the microgels together with the thermosensitive property can be utilised in recycling the catalyst, since the microgels can be filtered or centrifuged from the dispersion. While LCST-type thermosensitive behavior is utilised beneficially in many polymer and microgel applications, for catalytic applications the gel collapse can be seen as a drawback as the diffusivity of the reactants is suppressed around and above the phase transition temperature leading to lowered catalytic activity.

Microgels that exhibit the opposite thermoresponse, "thermophilicity" or "positive thermosensitivity" due to their upper critical solution temperature (UCST)-type behaviour have also been reported.[16–23] The microgels that expand upon heating are mostly based on polyacrylamide (PAM) with a charged polymer such as poly(acrylic acid) (PAA)[16–22] or poly(2-acrylamide-2-methylpropanesulfonic acid) (PAMPS).[23] These polymers form associative complexes at low temperatures by intermolecular hydrogen bonding between the repeating units. With increasing temperature the strength of the associations decreases leading to the swelling of the microgels. As the interaction is largely dependent on the charges on the PAA or PAMPS units, the thermosensitive behaviour of these systems is highly sensitive to pH and ionic strength. The catalytic applications of the UCST-type thermosensitive microgels have not been studied as extensively as those of the LCST-type systems, but it has been observed[23] that the catalytic activity is enhanced with the opening of the network structure upon heating, opposite to what has been found for the LCST-type microgels.

The UCST behaviour of non-ionic polymers in water typically relies on intra- and/or intermolecular hydrogen bonding, for example by primary amide groups.[24] Due to the relatively low strength of the hydrogen bonds, the observed phase transition temperature in the case of linear polymers may vary greatly for example with the concentration, molar mass and structure of the polymer. This may lead to broad phase transition temperature intervals with large hysteresis upon heating and cooling or even complete disappearance of the phase transition. However, the UCST-type phase transition behaviour of non-ionic polymers broadens the scope of applications of stimuli-responsive polymers and for example poly(*N*-acryloylglycinamide) (PNAGA)[24–28] is a promising non-ionic polymer showing UCST-type behaviour in water and saline solutions. It

Department of Chemistry, University of Helsinki, P. O. Box 55, FIN-00014, HU, Finland. E-mail: sami.hietala@helsinki.fi

†Electronic supplementary information (ESI) available: UV-spectra and TGA plots of AgNP dispersions, calculation of surface area, reaction rates and catalyst kinetics plots. See DOI: 10.1039/c7py01950e

has been demonstrated that gold nanoparticles decorated with PNAGA chains undergo UCST-type transition and can be envisioned for example for biomedical applications,[28] copolymers of PNAGA with biotin monomers have been used to prepare thermoresponsive magnetic nanoparticles for bioseparations[29] and macroscopic PNAGA hydrogels have been shown to undergo reversible size changes in water and saline solutions[30] and used for controlled drug release.[31,32]

Herein, we report PNAGA microgels that display thermophilic behaviour in water. The microgels are prepared by utilising the phase transition behaviour of PNAGA by using subambient polymerization temperature that leads to the precipitation of the polymer. In the presence of a bifunctional crosslinker and surfactant, crosslinked microgel particles are formed instead of linear chains. The microgels can further be used to encapsulate AgNPs and their catalytic activity at different temperatures is studied using the reduction of 4-nitrophenol in the presence of $NaBH_4$.

Experimental

Materials

Glycinamide hydrochloride (Bachem) and acryloyl chloride (Sigma Aldrich) were used as received and the *N*-acryloylglycinamide (NAGA) monomer was prepared as described earlier.[33] *N*,*N*′-Methylenebis(acrylamide) (BIS), ammonium persulfate (APS), *N*,*N*,*N*′,*N*′-tetramethylethylenediamine (TEMED) and sodium dodecyl sulfate (SDS) (all from Merck) were used as received. *N*-Isopropyl acrylamide (NIPAM, Acros organics) was recrystallised from hexane. Other substances and solvents with the highest purity were used as received. Deionised (DI) water was used for synthesis and purification. Regenerated cellulose dialysis tubing used for polymer purification was from Orange Scientific, with a molecular weight cutoff of 3500 g mol^{-1}.

Synthesis of PNAGA microgels

Free radical precipitation polymerization was employed in the synthesis of the thermosensitive UCST-type microgels, shown in Scheme 1. For all syntheses, the total monomer concentration was 70 mM, APS and TEMED concentrations each 1 mM and SDS 4 mM. The general procedure for PNAGA microgel syntheses (exemplified by PNAGA–2%BIS microgels) was to add 440 mg NAGA, 10.2 mg BIS crosslinker, and 57.7 mg SDS to a 100 ml round bottom flask with a magnetic stirrer bar and dissolve in 50 ml deionized water. The flask was placed in ice bath and stirred at a rotation rate of 750 rpm. The solution was purged with nitrogen for one hour before the reaction was initiated by adding 5.81 mg TEMED, immediately followed by the addition of 11.4 mg APS. The reaction was allowed to carry on in an ice bath for 6 h, after which the flask was kept at 4 °C overnight and then exposed to air. For the synthesis of PNAGA microgels with 4% BIS, only the BIS to monomer ratio was varied. For the reference PNIPAM–2%BIS microgels, the procedure was the same except that the reaction temperature was 70 °C and the reaction was stopped after 6 h by cooling and exposure to air. All the resulting microgel solutions were purified by extensive dialysis against deionized water.

Silver nanoparticle (AgNP) synthesis

The procedure for the synthesis of AgNPs inside the microgels was adapted from ref. 12. Generally, the PNAGA microgel dispersions (25 ml, 2.8 mg ml^{-1}) were mixed with $AgNO_3$ aqueous solution (10 ml, 0.56 mg ml^{-1}) at room temperature and stirred at 50 °C for 24 h under a N_2 atmosphere before placing the dispersion in a dialysis bag and dialysed against deionized ice-water for 2 h to remove the free silver ions. The reduction of Ag^+ was then initiated by slowly adding fresh aqueous $NaBH_4$ solution (10 ml, 0.75 mg ml^{-1}, 19.8 mM) into the flask in an ice bath. The reaction was allowed to carry on at room temperature for 24 h before dialysis against deionized water. The methods of synthesizing Ag–PNIPAM microgels was the same as described above, but the mixing of $AgNO_3$ with PNIPAM microgels was done in an ice bath and the following dialysis process was conducted at room temperature. As a reference, AgNPs with SDS used as a stabilizer (SDS concentration: 2.16×10^{-3} M) (AgNP–SDS) in the reduction step were made according to a published procedure.[34] Afterwards, a part of the dispersions was freeze-dried to determine the microgel concentrations gravimetrically and their Ag content by TGA. The AgNP sizes were determined from TEM images and the resulting surface area of the AgNPs in microgels was calculated based on this information. A detailed procedure for the calculation is presented in the ESI.†

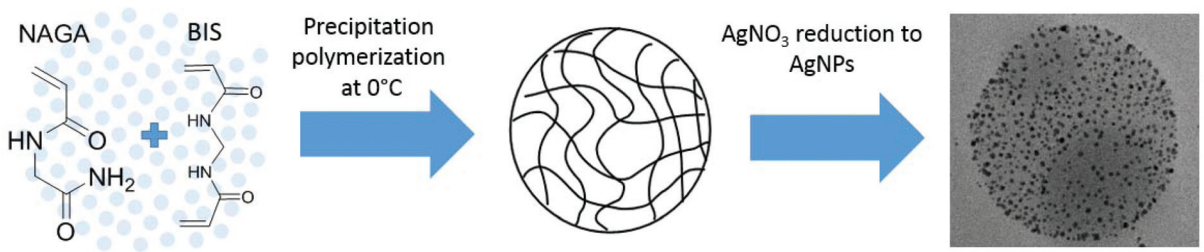

Scheme 1 Schematic illustration of the synthesis route to PNAGA microgels and Ag–PNAGA hybrid microgels.

Reduction of 4-nitrophenol

The reduction of 4-nitrophenol was conducted to study the catalytic properties of AgNPs containing dispersions at different temperatures. For each temperature, 4-nitrophenol (0.01 mg ml^{-1}, 0.072 mM) and fresh $NaBH_4$ (3.8 mg ml^{-1}, 100 mM) in 2.5 ml water were added to a standard 10 mm quartz cuvette. Then, 13 μl of the AgNP dispersion (microgel concentration after dialysis: Ag–PNAGA–2%BIS 0.74 mg ml^{-1}, Ag–PNAGA–4%BIS 1.49 mg ml^{-1} and Ag–PNIPAM–2%BIS 1.48 mg ml^{-1} and AgNP–SDS 0.08 mg ml^{-1}) was added to the cuvette and the UV-Vis absorbance at 400 nm was recorded. From the absorption data the induction time (t_0) indicated by no change in absorption was determined. The apparent reaction rate constant (k_{app}) was calculated from the changes of the absorbance at 400 nm after the induction time using the pseudo-first order kinetic equation, $\ln(c/c_0) = -k_{app}t$, where c_0 is the concentration at the beginning and c the concentration at time t.[4,35] Then, using the TGA data, the reaction rate was normalised to the Ag content of the microgels and further normalised with respect to the AgNP surface area employing the data from TEM image analysis. The reaction rate constant (k_1) normalised to the AgNP surface area was determined to enable a comparison between samples.[9] Details of the reaction rate constant calculations are given in the ESI.†

The catalytic reaction was also monitored during a temperature switch experiment between 50 °C and 5 °C. The quartz cuvette was charged with 2.5 ml aqueous solution of 4-nitrophenol (0.01 mg ml^{-1}) and $NaBH_4$ (3.8 mg ml^{-1}). The mixture was heated to 50 °C and 13 μl diluted AgNP dispersion was added. The change of absorbance at 400 nm was monitored for 5 min after which the sample compartment was cooled to 5 °C with the maximum cooling rate (~8 °C min^{-1}) of the instrument. The catalytic reaction was then monitored for 5 min at 5 °C and then the sample heated with the maximum heating rate (~15 °C min^{-1}), simultaneously monitoring the absorbance. The cycles were then repeated to observe the changes in catalytic activity.

Characterization

The sizes of the microgel particles were determined using dynamic light scattering (DLS) with Malvern Instruments Zetasizer Nano-ZS. For measurements the samples (concentration: 1 mg ml^{-1}) were passed through 0.45 μm Millipore PVDF filters prior to cell filling. The effective (Z-average) diameters were obtained from the second order cumulant fit and the size distributions using the Malvern inbuilt multiexponential fit. The nominal heating and cooling rate in the experiments was 10 °C h^{-1}. The UV-Vis spectra of the Ag-microgels as well as the changes in 4-nitrophenol spectra were recorded on a Shimadzu UV-1601 spectrometer equipped with a circulating thermostatted bath. The catalytic activity studies were performed using a Jasco J-815 CD spectrometer equipped with a Peltier controlled temperature accessory monitoring 400 nm absorbance and measuring the sample temperature inside the cuvette. In both cases measurements were made in quartz cuvettes with a cell path of 10 mm. Variable temperature ^{1}H NMR spectra of the monomers and polymers were recorded on a 500 MHz Bruker Avance III spectrometer in D_2O. For the NMR studies, the samples were made to 10 mg ml^{-1} polymer concentration in neat D_2O. The spectra intensities at different temperatures were calculated by comparing the integral of the solvent signal to the polymer signals. Thermogravimetric analysis (TGA) measurements were performed using Mettler Toledo 850 equipment. Samples were placed in 70 μl Al_2O_3 crucibles and heated from 25 °C to 800 °C at a heating rate of 10 K min^{-1} under a N_2 atmosphere. For PNAGA samples, runs were additionally made with a program that further kept the samples isothermally at 800 °C for two hours after the heating run due to the surprisingly high charred content even at 800 °C. TEM measurements were carried out using a Hitachi FESEM S-4800 electron microscope or a FEI Tecnai F20 Field Emission Gun 200 kV transmission electron microscope. The microgel samples were placed on a 300 mesh Cu grid with a uniform carbon film and dried at ambient temperature.

Results and discussion

Microgel synthesis

Free radical precipitation polymerization of NAGA in water at 0 °C in the presence of the BIS crosslinker was used to prepare thermosensitive PNAGA microgels (see Scheme 1). The precipitation polymerization is based on the solubility differences of the NAGA monomer and the resulting polymer, PNAGA. NAGA is water-soluble at all temperatures, while PNAGA precipitates at temperatures below its phase transition temperature. According to the literature, the phase transition temperature of linear PNAGA varies greatly,[24] but for example PNAGA with sufficiently high molar mass in a 1 wt% aqueous solution shows phase transition at 22–23 °C.[26] Thus, precipitation polymerization based microgel synthesis widely employed for LCST-type polymers, such as PNIPAM or poly(*N*-vinylcaprolactam) (PVCL), was adapted for a UCST-type polymer. This strategy produced reproducible PNAGA microgels with an average diameter of around 60 nm at room temperature and with a positive temperature response (see Fig. 1 and 2). The crosslinker concentration, 2 or 4 mol% with respect to the monomer, did not change markedly the phase transition behaviour or the size of the microgels as shown in Fig. 1. A higher crosslinker concentration, 6 mol%, produced a highly aggregated dispersion. Attempts at polymerizing NAGA in the absence of SDS on the other hand led to micrometer sized particles with a broad size distribution. Though these particles were also thermosensitive, further attempts at characterizing them were not made. In order to have a material as a reference to the catalysis studies, a PNIPAM microgel crosslinked with 2% BIS was prepared at 70 °C under corresponding synthesis conditions.

Thermosensitive properties

LCST-type polymer microgels shrink upon heating above their volume phase transition temperature (VPTT). An opposite

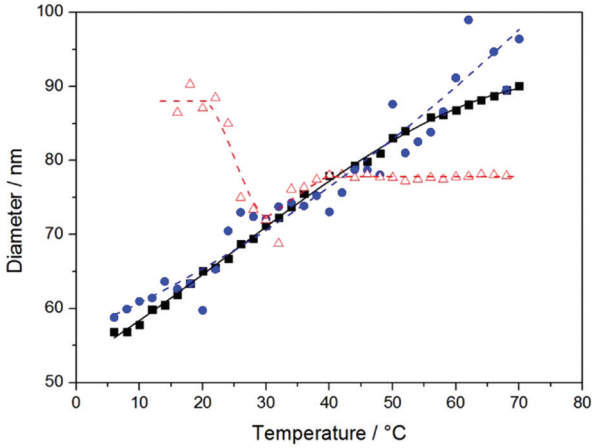

Fig. 1 The size of (■) PNAGA–2%BIS (●), PNAGA–4%BIS and (△) PNIPAM–2%BIS microgels upon heating based on DLS.

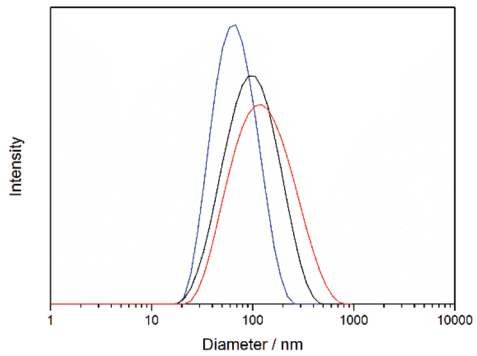

Fig. 2 Size distributions from DLS of the PNAGA–2%BIS microgel at 10 °C, 40 °C and 70 °C.

temperature effect, swelling upon heating, takes place for UCST-type microgels such as PAA–PAM.[18–20] However, often the UCST-type phase transitions are more sensitive to the polymer structure and environmental parameters than the LCST-type transitions. The UCST-type phase transition of even linear polymers often occurs over a very broad temperature range and may vary or even disappear depending on the pH, ionic strength or nature of the ionic species. For the PNAGA microgel dispersions in water in the present study it can be observed that the size of the microgels increases continuously upon heating up to 70 °C (see Fig. 1 and 2). For PNAGA–4%BIS the diameter increases about 1.5 times from 10 °C to 70 °C which equals to a 4-fold volume change (Table 1). The size changes for the PNAGA microgels were repeatable for three consecutive heating and cooling runs. Similar continuous swelling and shrinking behaviour has been observed for macroscopic BIS crosslinked PNAGA hydrogels in water and saline solutions.[30] In the case of macroscopic gels the increase of the amount of the BIS crosslinker lowered the degree of swelling, while in the case of these microgels the amount of the crosslinker does not appear to change the swelling significantly. An explanation to this behaviour may come from the

Table 1 Microgel properties

	Diameter 20 °C [nm]	Diameter 70 °C [nm]	Volume change [V(70 °C)/V(20 °C)]
PNAGA–2%BIS	65	90	2.7
PNAGA–4%BIS	60	96	4.1
PNIPAM–2%BIS	87	78	0.7

fact that during the precipitation polymerization the reactivity of the BIS crosslinker is typically higher than that of the monomer,[36] leading to a gradient in the crosslinking density from the core to the surface of the microgel particles, and, depending on the conversion, also to different final crosslinker/monomer ratios of the final particles.[37] For example for poly(*N*-isopropylmethacrylamide) microgels with varying crosslinker concentrations the diameter and swelling ratio first decreased with increased crosslinker concentration before the swelling ratio increased again.[38]

The size changes observed by DLS measurements are supported by variable temperature ^{1}H NMR experiments (see Fig. 3). The signals from the PNAGA microgel are nearly completely suppressed at low temperatures and intensify upon heating. This behavior results from the gradual dissociation of the hydrogen bonds upon heating leading to higher chain mobility and correspondingly more intense signals. As a comparison, the signal intensities of the PNIPAM microgel are plotted in the inset showing the loss of signal intensity at the phase transition temperature.

The lack of sharp volume phase transition in the PNAGA microgel size implies that upon the change of temperature the interactions in these microgels change gradually. Similar continuous swelling behaviour upon heating has also been reported for other thermophilic microgels, for example those based on PAA–PAM copolymers. However, an important aspect to consider with the PNAGA microgels is their phase transition behaviour compared to linear PNAGA polymers. For linear PNAGA, phase transition temperature is very sensitive to a number of parameters, including the concentration and molar

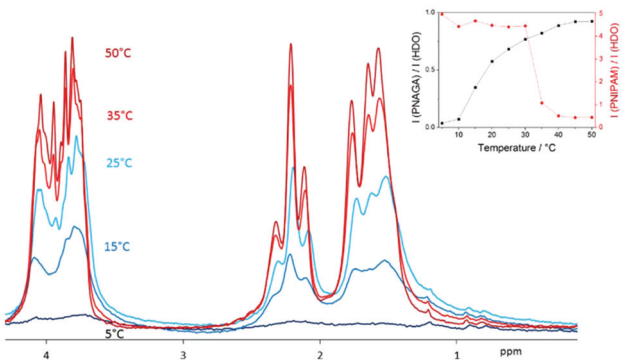

Fig. 3 Variable temperature ^{1}H NMR signals of the PNAGA–4%BIS microgel in D_2O. Inset: Corresponding integrated signal intensity at different temperatures compared with the solvent (HDO) signal. (■) PNAGA–4%BIS and for comparison (●) PNIPAM–2%BIS.

mass distribution of the polymer. In particular, the use of ionic initiators or ionic groups present in linear PNAGA has been shown to lower or suppress the thermosensitive property in water, in some cases leading to complete disappearance of the phase transition behaviour.[24,26,39] In the present case, despite the sulfate groups of the initiator fragments and the use of an anionic surfactant, the microgels show thermosensitive behaviour.

Synthesis of AgNPs inside the microgels

For the synthesis of AgNPs, the microgel dispersions were first incubated in $AgNO_3$ solution to load the silver ions inside the microgels and then dialysed to remove free ions which could contaminate the sample with AgNPs outside the microgels. To have the microgels in a swollen state, the incubation was performed at 50 °C for PNAGA and in an ice bath for PNIPAM. After dialysis, the reduction of Ag^+ ions to AgNPs was done in an ice bath through the addition of fresh $NaBH_4$. Upon the addition of $NaBH_4$ the dispersions turned instantly yellow indicating the formation of AgNPs. The sizes of the microgels slightly increased after the nanoparticle formation, but the microgels retained their temperature sensitivity (see Fig. 4). Somewhat surprisingly the DLS data for Ag–PNAGA–4%BIS show a larger increase in size than for Ag–PNAGA–2%BIS. A similar size increase with respect to the amount of the crosslinker used has been observed for PS–PNIPAM core–shell particles, where a higher amount of the crosslinker (5% or 10% BIS) leads to a larger size increase upon AgNP formation compared to the sample with 2.5% BIS.[9] At the moment the reason for this behaviour is unknown, but the heterogeneous distribution of the crosslinker inside the microgels resulting from the precipitation polymerization may lead to the observed difference in their swelling characteristics upon AgNP formation.

The TEM images of the PNAGA microgels and the AgNP containing samples are shown in Fig. 5. The images of the PNAGA microgels before AgNP addition (Fig. 5A and C) correspond well to the size shown by DLS. The AgNP containing Ag–PNAGA microgels (Fig. 5B and D) show similarly microgels agreeing with the size determined by DLS. The AgNP particles

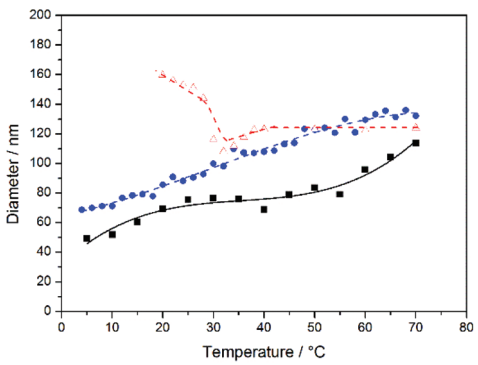

Fig. 4 The size according to DLS of (■) Ag–PNAGA–2%BIS (●) Ag–PNAGA–4%BIS and (△) Ag–PNIPAM–2%BIS microgels upon heating.

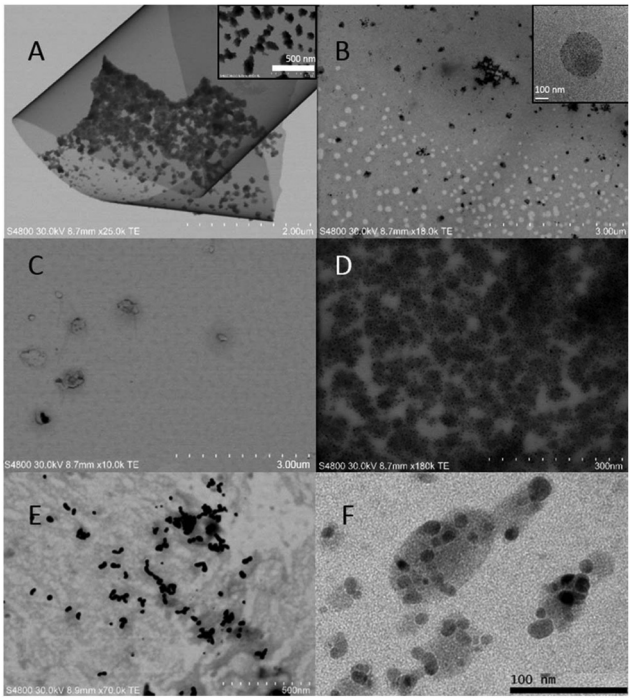

Fig. 5 TEM migrographs of (A) PNAGA–2%BIS, (B) Ag–PNAGA–2%BIS, (C) PNAGA–4%BIS, (D) Ag–PNAGA–4%BIS, (E) AgNP–SDS and (F) Ag–PNIPAM–2%BIS.

in the microgels (Fig. 5B, D and F) are shown as dark spots with a size below 10 nm. As can be seen, the AgNPs are generally encapsulated inside the microgels and correspond well to those found earlier for core–shell PS–PNIPAM based hybrid microgels (Table 2).[9] The presence of AgNPs was also determined by UV-Vis measurements. The UV-Vis spectra of all hybrid microgels show the typical surface plasmon resonance of AgNPs centered at 400 nm (Fig. S1†). The broadness of the signals indicates certain polydispersity of the AgNPs. However, the TEM images of the Ag–PNAGA microgels (Fig. 5B and D) show that the AgNPs are rather evenly distributed within the microgels and there is no clear size or concentration variation of the AgNPs from the core to the surface of the Ag–PNAGA microgels. Thus, the size variation of the AgNPs originates most likely from differences for example of the mesh size of the polymer network during the AgNP formation. When comparing the Ag–PNAGA–2%BIS and Ag–PNAGA–4%BIS microgels, the higher crosslinker amount led to the reduced average size of the AgNPs as could be expected for a more densely crosslinked network. At the same time, increasing the crosslinker concentration from 2% to 4% decreased the silver loading significantly (TGA; Table 2 and Fig. S2†). In order to enable the comparison of the catalytic efficiency between the different microgels, gravimetric data and TEM images were used to calculate the surface area of the Ag nanoparticles. As a comparison to the microgel based AgNP dispersions, AgNPs with only SDS (AgNP–SDS) as the stabilising agent were prepared. According to TEM (Fig. 5E), the size of the AgNP–SDS

Table 2 Properties of the AgNP microgels

	AgNP content[a] [wt%]	AgNP size[b] [nm]	AgNP surface area[c] [nm^2]
Ag–PNAGA–2%BIS	12.5	6.2 ± 1.7	1.1×10^{19}
Ag–PNAGA–4%BIS	7.7	4.7 ± 1.9	8.1×10^{18}
Ag–PNIPAM–2%BIS	4.4	8.6 ± 2.5	2.7×10^{18}
AgNP–SDS	0.008[d]	25.1 ± 7.5	2.1×10^{19}

[a] TGA. [b] TEM image analysis. [c] In 1 g of dry sample. [d] Ag content in dispersion, estimated assuming full conversion of $AgNO_3$ to AgNPs.

particles is bigger and they are more polydisperse than the AgNPs in the microgels, most likely due to the fact that no network was limiting the growth of the particles.

AgNP microgels as catalysts

To study the catalytic activity, a widely employed model reaction, reduction of 4-nitrophenol in the presence of $NaBH_4$,[40] was followed by UV-Vis measurements at different temperatures. The catalytic activity of the hybrid microgels and AgNP–SDS was compared by adding the samples into the 4-nitrophenol–$NaBH_4$ solution. The typical changes in the 4-nitrophenol absorption spectra are shown in Fig. S3† – the 400 nm absorbance was chosen as the reference wavelength for monitoring the kinetics. Upon addition of the AgNP containing microgels, the temperature, microgel structure and concentration were all found to contribute to the catalysis kinetics. For the hybrid microgels the reaction begins only after a certain induction time (Fig. 6 and 7, Fig. S4 and S5†) which is related to the temperature and the microgel in question. At temperatures below 20 °C, the induction time for Ag–PNAGA microgels is considerably longer than in the case of the Ag–PNIPAM–2%BIS microgel. This is due to the collapsed structure of Ag–PNAGA microgels that hinders the diffusion of reactants inside. Upon heating the induction times shorten for all microgels and for temperatures above 30 °C the induction times are only of the order of ten seconds for most of the studied reactions. For AgNP–SDS the reaction starts instantaneously regardless of temperature due to the more accessible Ag surfaces (Fig. S6†).

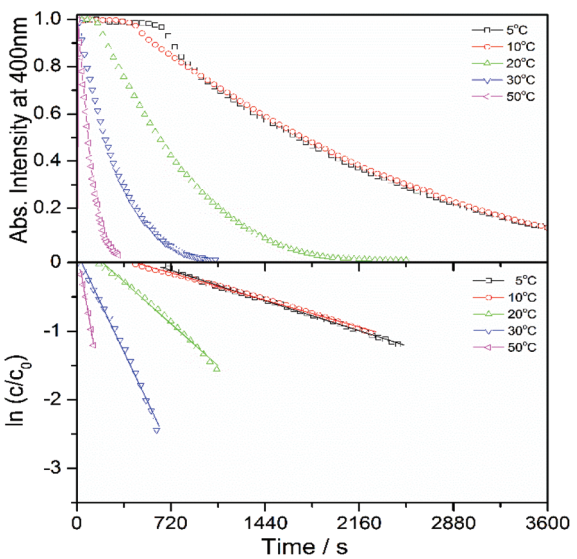

Fig. 6 Kinetics of 4-nitrophenol reduction with addition of the Ag–PNAGA–4%BIS microgel monitored by UV-Vis.

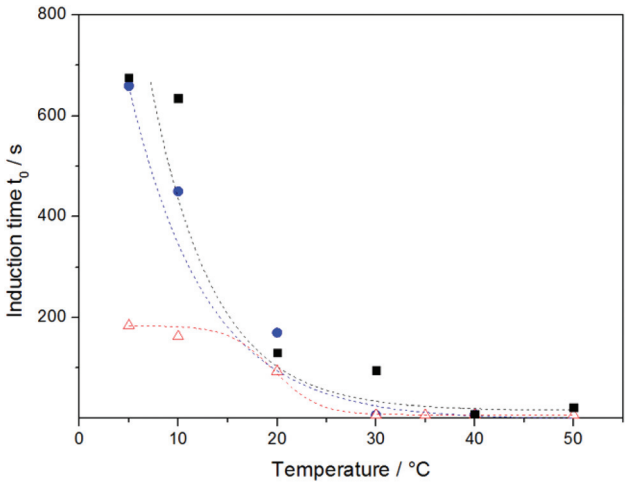

Fig. 7 Induction times of 4-nitrophenol reduction after different microgel injections. (■) Ag–PNAGA–2%BIS, (●) Ag–PNAGA–4%BIS and (△) Ag–PNIPAM–2%BIS. Lines are to guide the eye only.

In all the studied reactions, after exceeding t_0 the absorption from 4-nitrophenol begins to decay obeying pseudo-first order kinetics (see Fig. 6 and the ESI†). By analysing the linear part of the kinetic plots of $\ln(c/c_0)$ *versus* time, the apparent rate constants, k_{app}, for the reduction were determined for the respective dispersions. The mass and the size of the AgNPs were then used to normalise the rate constants to the Ag surface area, k_1 (Fig. 8 and Fig. S7†).

When observing the temperature dependence of the catalysis kinetics of Ag–PNIPAM–2%BIS in Fig. 8, it can be seen that at 35 °C, *i.e.* around the VPTT of PNIPAM, the catalytic efficiency is slightly reduced until the reaction rate starts to increase again at higher temperatures. This phenomenon has been observed before for PNIPAM based AgNP microgels[1,9,10] and is related to the shrinking of the microgels which reduces the diffusion of reactants inside.

When the reaction rates of the hybrid microgels are compared, it can be seen that the Ag–PNAGA microgels have generally higher apparent rate constants k_{app} than Ag–PNIPAM–2% BIS. This result is expected, as the Ag–PNAGA microgels have higher AgNP loading and smaller AgNP size. When the data are normalised to the AgNP surface area, the rate constants are generally on a comparable level for all microgels at room temperature. The k_1 values obtained for the Ag–PNIPAM–2%BIS microgel are similar to those reported earlier for core–shell type PS–PNIPAM Ag-microgels.[9] However, due to the different thermal responses of PNAGA and PNIPAM microgels, two observable trends are evident. Firstly, at low temperatures, the PNAGA microgels have lower reaction rate and also longer t_0

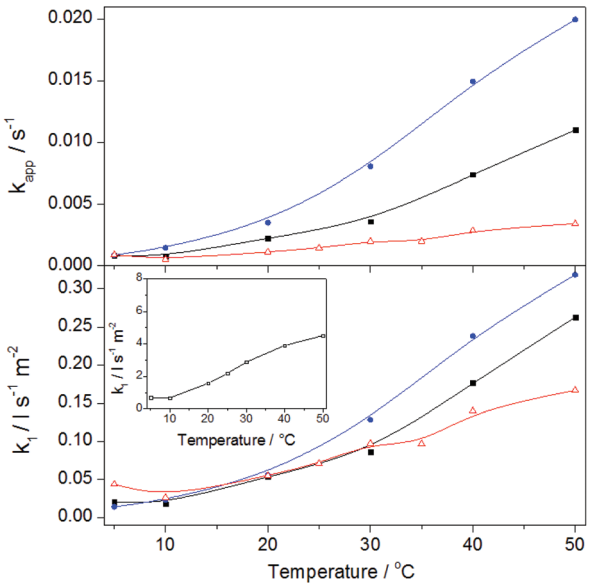

Fig. 8 Apparent (k_{app}) and normalised rate constants (k_1) of 4-nitrophenol reduction *vs.* temperature. Symbols: (■) Ag–PNAGA–2%BIS, (●) Ag–PNAGA–4%BIS and (△) Ag–PNIPAM–2%BIS and inset (□) for AgNP–SDS. The Arrhenius presentation of the normalised rate constant data is shown in Fig. S7.†

compared to PNIPAM due to the restricted diffusion inside the microgels. Secondly, at temperatures above 30 °C, the catalytic efficiency of Ag–PNAGA microgels increases significantly due to the expansion of the microgel networks and thus they show higher catalytic efficiency than PNIPAM. The differences in k_1 between the two Ag–PNAGA microgels may relate to the fact that the smaller size of AgNPs in Ag–PNAGA–4%BIS facilitates faster catalysis kinetics (specific turnover frequency, TOF) even when the data are normalised to the surface area.[9] The AgNP–SDS dispersions exhibit faster reaction rates compared to all the microgel samples (Fig. S6 and S7†). This is due to the thin SDS layer on the surface of the AgNPs.

The thermoreversible swelling behavior of the PNAGA microgels gives an additional possibility to tune the catalytic activity by modifying the diffusion by temperature. When the Ag–PNAGA–4%BIS microgel dispersion is injected to the reactant mixture at 50 °C (Fig. 9), as expected the reduction process begins almost instantaneously. However, when the mixture is cooled, the lowered temperature as well as the shrinking of the microgels slows down the reaction rate during the cooling and essentially switches the reaction off at 5 °C for a period of time. The catalytic activity can then be conveniently switched back to the "on" state by heating the mixture again and to the "off" state by cooling the mixture. As shown in Fig. S8,† a similar "off" state upon cooling is not observed for SDS stabilised AgNPs. We foresee that these hybrid thermophilic microgels may be utilised in the future for efficient and more complex catalytic transformations and for advanced control over the catalytic processes.

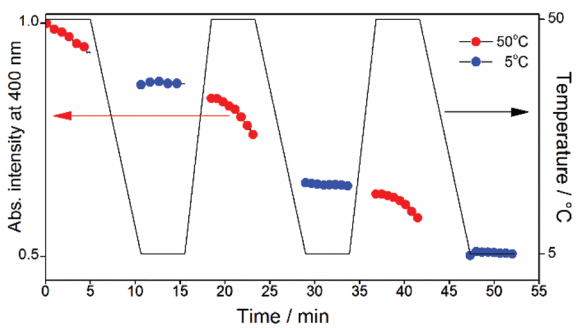

Fig. 9 The decrease of 4-nitrophenol absorbance *versus* time while changing the temperature. Microgel: Ag–PNAGA–4%BIS; concentration: 0.0149 mg ml^{-1}.

Conclusions

Thermosensitive poly(*N*-acryloylglycinamide) (PNAGA) microgels were prepared by aqueous precipitation polymerization. By utilising polymerization temperature lower than the UCST of PNAGA, successful microgel preparation was accomplished. The PNAGA microgels swelled upon heating in water leading to over a 4-fold increase in the volume upon heating from 5 °C to 70 °C in the case of the PNAGA–4%BIS microgel. Hybrid microgels containing silver nanoparticles were prepared by reducing $AgNO_3$ inside them. These hybrid microgels retained the thermosensitive behaviour and were shown to catalyse the reduction of 4-nitrophenol in aqueous dispersion. Upon heating the catalytic efficiency of PNAGA microgels increased more when compared to the LCST-type poly(*N*-isopropyl acrylamide) (PNIPAM) microgel. This enhancement originates from the increased diffusivity of reactants in the swollen PNAGA microgel. The thermosensitive behaviour of PNAGA microgels was shown to allow them to have control over their catalytic activity upon change of temperature.

Conflicts of interest

There are no conflicts to declare.

Acknowledgements

Dong Yang acknowledges the China Scholarship Council PhD grant number 201506950008. The Electron Microscopy Unit of the University of Helsinki is acknowledged for the TEM images.

Notes and references

1 M. Ballauff and Y. Lu, *Polymer*, 2007, **48**, 1815–1823.
2 N. Welsch, M. Ballauff and Y. Lu, in *Chemical Design of Responsive Microgels*, ed. A. Pich and W. Richtering, Springer-Verlag Berlin, Berlin, 2010, vol. 234, pp. 129–163.

3 J. B. Thorne, G. J. Vine and M. J. Snowden, *Colloid Polym. Sci.*, 2011, **289**, 625.
4 R. Begum, K. Naseem and Z. H. Farooqi, *J. Sol-Gel Sci. Technol.*, 2015, **77**, 497–515.
5 F. A. Plamper and W. Richtering, *Acc. Chem. Res.*, 2017, **50**(2), 131–140.
6 J. Zhang, M. Zhang, K. Tang, F. Verpoort and T. Sun, *Small*, 2014, **10**, 32–46.
7 J. Zhang, S. Xu and E. Kumacheva, *J. Am. Chem. Soc.*, 2004, **126**, 7908–7914.
8 Y. Lu, Y. Mei, M. Drechsler and M. Ballauff, *Angew. Chem., Int. Ed.*, 2006, **45**, 813–816.
9 Y. Lu, Y. Mei, M. Ballauff and M. Drechsler, *J. Phys. Chem. B*, 2006, **110**, 3930–3937.
10 Y.-Y. Liu, X.-Y. Liu, J.-M. Yang, D.-L. Lin, X. Chen and L.-S. Zha, *Colloids Surf., A*, 2012, **393**, 105–110.
11 Z. H. Farooqi, K. Naseem, R. Begum and A. Ijaz, *J. Inorg. Organomet. Polym. Mater.*, 2015, **25**, 1554–1568.
12 Y. Tang, T. Wu, B. Hu, Q. Yang, L. Liu, B. Yu, Y. Ding and S. Ye, *Mater. Chem. Phys.*, 2015, **149–150**, 460–466.
13 A. Biffis, S. Cunial, P. Spontoni and L. Prati, *J. Catal.*, 2007, **251**, 1–6.
14 S. Carregal-Romero, N. J. Buurma, J. Pérez-Juste, L. M. Liz-Marzán and P. Hervés, *Chem. Mater.*, 2010, **22**, 3051–3059.
15 S. Shi, L. Zhang, T. Wang, Q. Wang, Y. Gao and N. Wang, *Soft Matter*, 2013, **9**, 10966.
16 P. Bouillot and B. Vincent, *Colloid Polym. Sci.*, 2000, **278**, 74–79.
17 D. E. Owens, Y. Jian, J. E. Fang, B. V. Slaughter, Y.-H. Chen and N. A. Peppas, *Macromolecules*, 2007, **40**, 7306–7310.
18 C. Echeverria, D. López and C. Mijangos, *Macromolecules*, 2009, **42**, 9118–9123.
19 C. Echeverria and C. Mijangos, *Macromol. Rapid Commun.*, 2010, **31**, 54–58.
20 C. Echeverria and C. Mijangos, *Langmuir*, 2011, **27**, 8027–8035.
21 C. Echeverria, N. A. Peppas and C. Mijangos, *Soft Matter*, 2012, **8**, 337–346.
22 A. G. Alvarado, J. Cortés, L. A. Pérez-Carrillo, M. Rabelero, J. Arellano, J. C. Sánchez-Díaz, J. E. Puig and M. Arellano, *J. Macromol. Sci., Part B: Phys.*, 2016, **55**, 1086–1098.
23 S. Li, Y. Ge, A. Tiwari and S. Cao, *Small*, 2010, **6**, 2453–2459.
24 J. Seuring and S. Agarwal, *Macromol. Rapid Commun.*, 2012, **33**, 1898–1920.
25 H. Haas and N. Schuler, *J. Polym. Sci., Part B: Polym. Lett.*, 1964, **2**, 1095.
26 J. Seuring, F. M. Bayer, K. Huber and S. Agarwal, *Macromolecules*, 2012, **45**, 374–384.
27 J. Seuring and S. Agarwal, *Macromol. Chem. Phys.*, 2010, **211**, 2109–2117.
28 F. Liu and S. Agarwal, *Macromol. Chem. Phys.*, 2015, **216**, 460–465.
29 N. Ohnishi, H. Furukawa, H. Hideyuki, J.-M. Wang, C.-I. An, E. Fukusaki, K. Kataoka, K. Ueno and A. Kondo, *Nanobiotechnology*, 2006, **2**, 43–49.
30 F. Liu, J. Seuring and S. Agarwal, *Macromol. Chem. Phys.*, 2014, **215**, 1466–1472.
31 M. Boustta, P.-E. Colombo, S. Lenglet, S. Poujol and M. Vert, *J. Controlled Release*, 2014, **174**, 1–6.
32 M. Boustta and M. Vert, *Drug Delivery Transl. Res.*, 2017, **7**, 460–464.
33 L. Mäkinen, D. Varadharajan, H. Tenhu and S. Hietala, *Macromolecules*, 2016, **49**, 986–993.
34 T. Pal, T. K. Sau and N. R. Jana, *Langmuir*, 1997, **13**, 1481–1485.
35 R. Begum, K. Naseem, E. Ahmed, A. Sharif and Z. H. Farooqi, *Colloids Surf., A*, 2016, **511**, 17–26.
36 X. Wu, R. H. Pelton, A. E. Hamielec, D. R. Woods and W. McPhee, *Colloid Polym. Sci.*, 1994, **272**, 467–477.
37 R. Acciaro, T. Gilányi and I. Varga, *Langmuir*, 2011, **27**, 7917–7925.
38 A. Guillermo, C. Addad, J. P. Bazile, D. Duracher, A. Elaissari and C. Pichot, *J. Polym. Sci., Part B: Polym. Phys.*, 2000, **38**, 889–898.
39 J. Niskanen and H. Tenhu, *Polym. Chem.*, 2017, **8**, 220–232.
40 T. Aditya, A. Pal and T. Pal, *Chem. Commun.*, 2015, **51**, 9410–9431.